

# Control of Multistability through Local Sensitivity Analysis: Application to Cellular Decision-making Networks

Rodrigo Moreno-Morton<sup>†1</sup> and Alessio Franci<sup>†2</sup>

**Abstract**—Control of multistable dynamical system has important applications, from physics to biology. Here, we attack this problem from the perspective of local sensitivity analysis. We develop *local* sensitivity rules to control *global* properties of continuous-time multistable dynamics with simple attractors, namely, the relative size and depth of their basins of attraction. Our parameter control signal is computationally cheap and provides counter-intuitive information about the sensitive parameters to be manipulated in an experimental setting.

## I. INTRODUCTION

Multistable dynamics and their control appear in a variety of physical, engineered, and biological systems [1]. Opinion-formation and decision-making networks also exhibit multistability and are receiving increasing attention due to their relevance in sociopolitical systems and for collective behaviors in both biological and artificial agent groups. In these networks, each attractor corresponds to a decision state (see [2] and references therein). Another important example of multistable decision-making are molecular regulatory networks, where decisions correspond to cellular phenotypes [3]. Cellular decision-making can be functional, i.e., development, but also deleterious for the organism, i.e., tumor formation.

A well studied case of cellular decision-making with both functional or deleterious consequences is the epithelial-mesenchymal transition (EMT), a change in phenotype of epithelial cells from a clearly polarized, epithelium-adhered cell (epithelial phenotype) to a non-polarized, free-moving cell (mesenchymal phenotype) [4], [5]. EMT plays an important role in several stages of embryonic development and tissue repair but also in tumor metastasis [6]. Understanding how the EMT is regulated and how it may be controlled is relevant both for biology and medicine.

Global analysis and control of multi-stable dynamics are hard in general. Although almost global Lyapunov functions are known to exist for multistable systems [7], their analytical computation is impossible except for simple low-dimensional examples. Some local approaches, based on the model linearization, have been developed for discrete-time dynamical systems with chaotic dynamics [1].

Motivated by EMT control, in this paper we focus on multistable dynamics in which the only attractors are exponentially stable equilibria and in which the boundary of the basins of attraction are the stable manifolds of saddle points. We rigorously show that controlling two local system properties,

i.e., eigenvalues of the linearized dynamics and location of saddle points, controls the global organization of the basins of attraction. Based on these results, we derive algorithmic control strategies, based on local sensitivity analysis, to compute sensitive parameter directions to increase or decrease the relative size and depth of a given basin of attraction.

After having introduced the needed notation and definitions in Section II, we rigorously develop the theory for one-dimensional dynamics in Section III. In Section IV, we introduce the relevant class of high-dimensional multistable dynamics. We show how the one-dimensional theory applies to one-dimensional invariant sets given by the unstable manifolds of the saddle points. Dynamics on those invariant sets are key determinants of the model's multistability. We then formulate our control strategies algorithmically. The connection between the proposed control strategies, parameter sensitivity analysis, and (multi)gradient descent algorithms is also discussed. Section IV-F applies the proposed control strategies on a two-dimensional gradient dynamical system and illustrates the underlying mechanisms on the model phase plane. Section V briefly introduces a novel ODE model of the EMT regulatory network and applies the proposed control strategies to increase the size of the basin of attraction of the (healthy) epithelial state. Conclusions are summarized in Section VI.

## II. NOTATION AND DEFINITIONS

$\mathbb{R}$  denotes the set of real numbers.  $\mathbb{N}$  denotes the set of positive integers.  $\mathbb{C}$  denotes the set of complex numbers.  $\langle \cdot, \cdot \rangle : \mathbb{R}^n \times \mathbb{R}^n \rightarrow \mathbb{R}$  denotes the Euclidean product in  $\mathbb{R}^n$  and  $\|\cdot\| : \mathbb{R}^n \rightarrow \mathbb{R}$  its induced norm. Given  $x \in \mathbb{R}$ ,  $\text{sgn}(x)$  denotes its sign, i.e.,  $\text{sgn}(x) = -1$  if  $x < 0$ ,  $\text{sgn}(x) = 0$  if  $x = 0$ , and  $\text{sgn}(x) = 1$  if  $x > 0$ . Given  $z \in \mathbb{C}$ ,  $\text{Re}(z)$  denotes its real part. A set  $\mathcal{K} \subset \mathbb{R}^n$  is a linear cone if for all  $x \in \mathcal{K}$  and all  $a > 0$ ,  $ax \in \mathcal{K}$ . Given  $x \in \mathbb{R}^n$  a set  $\mathcal{K}_x$  is an affine cone with vertex at  $x$  if there exists a linear cone  $\mathcal{K}$  such that, for all  $v \in \mathcal{K}_x$ ,  $v = w + x$  with  $w \in \mathcal{K}$ .

Consider a smooth dynamical system

$$\frac{dx}{dt} =: \dot{x} = f(x), \quad f : \mathbb{R}^n \rightarrow \mathbb{R}^n. \quad (1)$$

with flow  $\varphi : \mathbb{R}^n \times \mathbb{R} \rightarrow \mathbb{R}^n$ , i.e., given  $y \in \mathbb{R}^n$ ,  $x(t) = \varphi(y, t)$  is the solution of (1) at time  $t$  with initial conditions  $x(0) = y$ . An equilibrium  $x^*$  of (1) is called hyperbolic if the Jacobian  $\frac{\partial f}{\partial x}(x^*) \in \mathbb{R}^{n \times n}$  has no eigenvalues on the imaginary axis. The stable manifold of an equilibrium  $x^*$  is the set  $\{x \in \mathbb{R}^n : \lim_{t \rightarrow \infty} \varphi(x, t) = x^*\}$ . The unstable manifold of an equilibrium  $x^*$  is the set  $\{x \in \mathbb{R}^n : \lim_{t \rightarrow -\infty} \varphi(x, t) = x^*\}$ . If a hyperbolic equilibrium  $x^*$  is stable, that is, if  $\frac{\partial f}{\partial x}(x^*)$  has only eigenvalues with negative real part, then its stable manifold is called its basin

This work was supported by DGAPA-PAPIIT(UNAM) grant n. IN102420 and Conacyt CB grant n. A1-S-10610.

<sup>†</sup> Math Department at the Faculty of Sciences, National Autonomous University of Mexico (UNAM).

<sup>1</sup> luiomormor@gmail.com

<sup>2</sup> afranci@ciencias.unam.mx

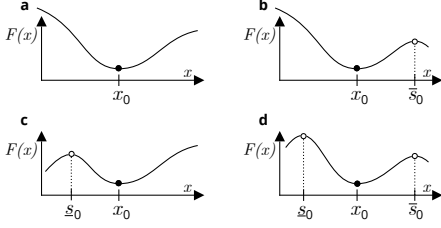


Fig. 1: Unbounded vs bounded one-dimensional basins of attraction. **a.** Unbounded. **b,c.** Half-bounded. **d.** Bounded. Stable equilibria are denoted by dots; unstable equilibria by circles.

of attraction. A set  $U \subset \mathbb{R}^n$  is called invariant for model (1) if  $x \in U$  implies  $\varphi(x, t) \in U$  for all  $t \in \mathbb{R}$ .

### III. ONE-DIMENSIONAL THEORY

Consider a one-dimensional dynamical system

$$\dot{x} = f(x) = -F'(x) \quad (2)$$

where  $f : \mathbb{R} \rightarrow \mathbb{R}$  is smooth and  $F$  is a primitive of  $-f$ , i.e.,  $F(x) = -\int_0^x f(y)dy + C$ ,  $C \in \mathbb{R}$ . Observe that  $F(x)$  is an almost global Lyapunov function for (2), in the sense of [7]. Suppose that  $x_0$  is an exponentially stable equilibrium of (2), that is,

$$F'(x_0) = 0, \quad F''(x_0) > 0. \quad (3)$$

Generically there are three possible cases for the geometry of the basin of attraction of  $x_0$ : unbounded (Figure 1a), half-bounded (Figure 1b,c), bounded (Figure 1d). Boundaries of the basin of attraction, when they exist, are given by unstable points  $\underline{s}_0$ ,  $\bar{s}_0$ , with  $\underline{s}_0 < x_0 < \bar{s}_0$ , satisfying<sup>1</sup>

$$F'(\underline{s}_0) = F'(\bar{s}_0) = 0, \quad F''(\underline{s}_0), F''(\bar{s}_0) < 0. \quad (4)$$

We focus on the bounded case (Figure 1d) but we also remark that our theoretical developments apply naturally to the bounded side of the half-bounded cases (Figure 1b,c).

Our goal is understanding how the presence of possible control parameters in model (2) affect the depth (i.e., local stability) and size of the basin of attraction of  $x_0$ , as well as understanding how depth and size can be related.

#### A. Enhancing local stability of $x_0$ increases the size of its basin of attraction

Suppose there is a parameter  $\alpha$  that tunes the local stability of  $x_0$  as

$$\dot{x} = -F'(x) - \kappa(x, \alpha) \quad (5)$$

where  $\kappa : \mathbb{R} \times \mathbb{R} \rightarrow \mathbb{R}$  is smooth and satisfies

$$\begin{aligned} \kappa(x, 0) = 0, \quad \text{sgn} \left( \frac{\partial \kappa}{\partial x}(x, \alpha) \right) &= \text{sgn}(\alpha), \\ \text{sgn} \left( \frac{\partial \kappa}{\partial \alpha}(x, 0) \right) &= \text{sgn}(x - x_0). \end{aligned} \quad (6)$$

As representative examples,  $\kappa(x, \alpha) = \alpha(x - x_0)$  or  $\kappa(x, \alpha) = \alpha \bar{\kappa}(x)$  with  $\bar{\kappa}(\cdot)$  strictly monotone increasing and  $\bar{\kappa}(x_0) = 0$ .

<sup>1</sup>We denote the unstable equilibria with an  $s$  because in higher dimension they will correspond to *saddle* points.

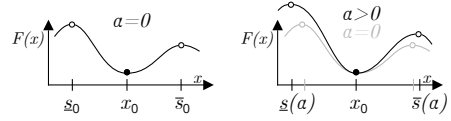


Fig. 2: Increasing the stability of an exponentially stable equilibrium increases the size of its basin of attraction, and vice-versa.

Observe that model (5) has almost global Lyapunov function  $V(x, \alpha) = F(x) + \int_0^x \kappa(y, \alpha)dy$ .

Increasing  $\alpha$  enhances the local stability of  $x_0$ , in the sense that  $\frac{\partial}{\partial \alpha} \frac{\partial \dot{x}}{\partial x} \Big|_{x=x_0} < 0$ , which implies  $\frac{\partial \dot{x}}{\partial x} \Big|_{x=x_0} < \frac{\partial \dot{x}}{\partial x} \Big|_{x=x_0} < 0$ , i.e., the eigenvalue of the linearization at  $x_0$  becomes more negative as  $\alpha$  is increased.

Let  $\underline{s}(\alpha)$  and  $\bar{s}(\alpha)$  be the boundaries of the basin of attraction of  $x_0$  for sufficiently small  $\alpha$ . In particular,  $\underline{s}(0) = \underline{s}_0$  and  $\bar{s}(0) = \bar{s}_0$ .

**Lemma III.1.** *The two functions  $\underline{s}(\alpha)$  and  $\bar{s}(\alpha)$  are differentiable at  $\alpha = 0$ . Furthermore  $\underline{s}'(0) < 0$  and  $\bar{s}'(0) > 0$ .*

*Proof.* By definition  $V'(\underline{s}(\alpha), \alpha) \equiv 0$  for  $\alpha$  sufficiently small. Differentiating with respect to  $\alpha$  we get

$$\left( F''(\underline{s}(\alpha)) + \frac{\partial \kappa}{\partial x}(\underline{s}(\alpha), \alpha) \right) \underline{s}'(\alpha) + \frac{\partial \kappa}{\partial \alpha}(\underline{s}(\alpha), \alpha) = 0. \quad (7)$$

Invoking (4) and (6), it follows that  $\underline{s}'(0) = -\frac{\partial \kappa}{\partial \alpha}(\underline{s}_0, 0)/F''(\underline{s}_0) < 0$ . Similarly, we get  $\bar{s}'(0) > 0$ . ■

The following theorem, illustrated in Figure 2, is a direct corollary of Lemma III.1.

**Theorem III.1.** *In model (5), enhancing the stability of  $x_0$ , that is, making  $\frac{\partial \dot{x}}{\partial x} \Big|_{x=x_0}$  more negative, by increasing  $\alpha$ , also increases the size of its basin of attraction.*

#### B. Increasing the basin of attraction of $x_0$ enhances its local stability

We can prove a converse result to Theorem III.1 in the case the model is linear in the parameter  $\alpha$ . Let  $\tilde{\kappa} : \mathbb{R} \rightarrow \mathbb{R}$  be monotone and consider

$$\dot{x} = -F'(x) - \alpha \tilde{\kappa}(x) \quad (8)$$

As above, let  $\underline{s}(\alpha)$  and  $\bar{s}(\alpha)$  be the boundary of the basin of attraction of  $x_0$  for sufficiently small  $\alpha$ .

**Lemma III.2.** *If  $\underline{s}(\alpha) < \underline{s}_0$  and  $\bar{s}(\alpha) > \bar{s}_0$  for  $\alpha > 0$ , then  $\tilde{\kappa}(\cdot)$  is monotone increasing on  $(\underline{s}_0, \bar{s}_0)$ . In particular  $\tilde{\kappa}'(x_0) > 0$  and*

$$\frac{\partial}{\partial \alpha} \frac{\partial \dot{x}}{\partial x} \Big|_{x=x_0} < 0. \quad (9)$$

*Proof.* Invoking (4) and (7), it follows that  $\tilde{\kappa}(\underline{s}(\alpha)) < 0$  and  $\tilde{\kappa}(\bar{s}(\alpha)) > 0$ . Hence, because  $\tilde{\kappa}$  is monotone, it is necessarily monotone increasing on  $(\underline{s}_0, \bar{s}_0)$ . To prove the second part of the statement, compute  $\frac{\partial}{\partial \alpha} \frac{\partial \dot{x}}{\partial x} \Big|_{x=x_0} = -\tilde{\kappa}'(x_0) < 0$ . ■

The following theorem is a direct corollary of Lemma III.2.

**Theorem III.2.** *In model (5), increasing the size of the basin of attraction of  $x_0$  by increasing  $\alpha$  also enhances the stability of  $x_0$ , in the sense that (9) holds.*

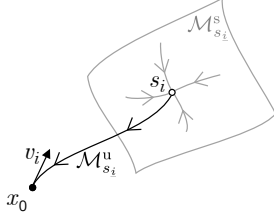


Fig. 3: The one-dimensional invariant dynamics over  $\mathcal{M}_{s_i}^u$  between a stable point  $x_0$  and a saddle point  $s_i$ , and associated eigenvector  $v_i$  at  $x_0$ .

#### IV. HIGH-DIMENSIONAL ALGORITHMIC GENERALIZATION

Our goal is to apply the results of the one-dimensional theory in Section III to higher-dimensional systems of the form

$$\dot{x} = F(x, \pi), \quad (10)$$

where  $x \in \mathbb{R}^n$ ,  $\pi \in \mathbb{R}^m$  is a vector of parameters, and  $F : \mathbb{R}^n \times \mathbb{R}^m \rightarrow \mathbb{R}^n$  is smooth.

**Definition IV.1.** An unstable equilibrium of model (10) is called a *saddle point* if its stable manifold is  $n-1$ -dimensional and an *unstable equilibrium* otherwise

**Assumption IV.1.** The only attractors of model (10) are exponentially stable equilibria with purely real simple eigenvalues. The basins of attractions of stable equilibria are separated by the union of the stable manifolds of saddle points.

Assumption IV.1 is generically satisfied, e.g., by gradient dynamical systems [8] and monotone systems [9].

Under Assumption IV.1, each stable equilibrium  $x_0 \in \mathbb{R}^n$  of model (10) is surrounded by a set of saddle points  $s_1, \dots, s_l \in \mathbb{R}^n$ ,  $l \leq n$ , and associated stable and unstable manifolds,  $\mathcal{M}_{s_i}^s$  and  $\mathcal{M}_{s_i}^u$ ,  $i = 1, \dots, l$ , respectively. The union  $\bigcup_{i=1}^l \mathcal{M}_{s_i}^s$  of the saddle stable manifolds defines the boundary of the basin of attraction of  $x_0$ . Each saddle unstable manifold  $\mathcal{M}_{s_i}^u$  is a one-dimensional invariant set connecting  $x_0$  and  $s_i$  (see Figure 3). Let

$$J_x^\pi = \frac{\partial F}{\partial x}(x, \pi) \quad (11)$$

be the Jacobian of model (10) at  $x$  and for parameters  $\pi$ . Then each  $\mathcal{M}_{s_i}^u$  is tangent at  $x_0$  to a distinct eigenvector  $v_i$  of  $J_{x_0}^\pi$  with associated eigenvalue  $\lambda_i < 0$ .

The rationale to apply the one-dimensional theory in Section III to model (10) is that it applies along each  $\mathcal{M}_{s_i}^u$ :

- Making the eigenvalue  $\lambda_i$  more negative will also push the saddle  $s_i$  (and associated stable manifold  $\mathcal{M}_{s_i}^s$ ) away from  $x_0$ , which enlarges its basin of attraction.
- Vice-versa, pushing  $s_i$  away from  $x_0$  will also make  $\lambda_i$  more negative.

Proving these ideas formally is very hard in general because of the difficulty of analytically define unstable manifolds. Here, we take instead an algorithmic approach to apply them in concrete cases and verify their efficacy *a posteriori*.

##### A. Two useful lemmas

The following basic lemmas provide the basic tools for eigenvalue and saddle location control.

**Lemma IV.1.** Let  $x^*$  be a hyperbolic equilibrium of (10), i.e.,  $F(x^*, \pi) = 0$ . Then  $\frac{\partial x^*}{\partial \pi_i} = -(J_{x^*}^\pi)^{-1} \frac{\partial F}{\partial \pi_i}(x^*, \pi)$ .

*Proof.* Because  $x^*$  is hyperbolic,  $J_{x^*}^\pi$  is not singular and the lemma follows by the implicit function theorem. ■

**Lemma IV.2.** Let  $x^*$  be a hyperbolic equilibrium of (10). Let  $\lambda \in \mathbb{C}$  be an eigenvalue of  $J_{x^*}^\pi$  with left eigenvector  $w \in \mathbb{C}^n$  and right eigenvector  $v \in \mathbb{C}^n$ . The total derivative  $D_i \lambda = \frac{\partial \lambda_i}{\partial x} \frac{\partial x^*}{\partial \pi_i} + \frac{\partial \lambda_i}{\partial \pi_i}$  of  $\lambda$  with respect to  $\pi_i$  is given by  $D_i \lambda = \frac{w^T D_i J_{x^*}^\pi v}{w^T v}$ , where  $D_i J_{x^*}^\pi$  is the total derivative of  $J_{x^*}^\pi$  with respect to  $\pi_i$ , i.e.  $D_i J_{x^*}^\pi = \frac{\partial J_{x^*}^\pi}{\partial x} \frac{\partial x^*}{\partial \pi_i} + \frac{\partial J_{x^*}^\pi}{\partial \pi_i}$ .

*Proof.* By differentiating the equality  $w^T J_{x^*}^\pi v = w^T \lambda v$  with respect to  $\pi_i$  and noticing that the terms involving derivatives of  $w^T$  and  $v$  cancel out, we obtain  $w^T \left( \frac{\partial J_{x^*}^\pi}{\partial x} \frac{\partial x^*}{\partial \pi_i} + \frac{\partial J_{x^*}^\pi}{\partial \pi_i} \right) v = w^T \left( \frac{\partial \lambda_i}{\partial x} \frac{\partial x^*}{\partial \pi_i} + \frac{\partial \lambda_i}{\partial \pi_i} \right) v$  and the result follows. ■

##### B. Eigenvalue control by local sensitivity analysis

Consider a stable equilibrium  $x_0$  of model (10) with parameters  $\pi$  and let Assumption IV.1 hold. Let  $\lambda < 0$  be an eigenvalue of  $J_{x_0}^\pi$  with left eigenvector  $w \in \mathbb{R}^n$  and right eigenvector  $v \in \mathbb{R}^n$ . Our goal is to make  $\lambda$  more negative through suitable parameter variation.

The gradient of  $\lambda$  with respect to the vector of parameter can be computed using Lemma IV.2 as

$$\nabla \lambda = [D_1 \lambda, \dots, D_m \lambda] = \left[ \frac{w^T D_1 J_{x^*}^\pi v}{w^T v}, \dots, \frac{w^T D_m J_{x^*}^\pi v}{w^T v} \right]$$

where  $D_i J_{x^*}^\pi = \frac{\partial J_{x^*}^\pi}{\partial x} \frac{\partial x^*}{\partial \pi_i} + \frac{\partial J_{x^*}^\pi}{\partial \pi_i}$  and  $\frac{\partial x^*}{\partial \pi_i}$  can be computed as in Lemma IV.1. The direction in the parameter space that leads to the fastest decrease of  $\lambda$  is therefore

$$d_\lambda = - \frac{\nabla \lambda}{\|\nabla \lambda\|}. \quad (12)$$

Suppose all parameters can be controlled independently and no other parametric constraints are present. The proposed control strategy to decrease  $\lambda$  by  $\delta \lambda > 0$  units is the following.  $0 < \varepsilon \ll 1$  and  $n_{ite} \in \mathbb{N}$  are control hyperparameters.

##### Control Strategy IV.1. Fully-Actuated Eigenvalue Control

1. Compute (12) at current equilibrium and parameter values.
2. Update the parameters:  $\pi \leftarrow \pi + \varepsilon d_\lambda$  and compute the new equilibrium points.
3. Repeat steps 1,2 until  $\lambda$  decreased by  $\delta \lambda$  or until the maximum number of iterations  $n_{ite}$  is exceeded.

There might be situations in which not all parameters in  $\pi$  can be controlled independently (e.g., some could not be controlled at all) or other constraints are present on the directions along which  $\pi$  can be modulated (e.g., optimizing other control objectives).

We assume that admissible directions along which parameters can be controlled at  $\pi$  form an affine cone  $\mathcal{K}_\pi \subset \mathbb{R}^m$ . The resulting control strategy is as follow.

### Control Strategy IV.2. Underactuated Eigenvalue Control

1. Compute  $\tilde{d}_\lambda = \arg \max_{d \in \mathcal{K}_\pi} \frac{\langle d, d_\lambda \rangle}{\|d\|}$  at current equilibrium and parameter values.
2. Update the parameters:  $\pi \leftarrow \pi + \varepsilon d$  and compute the new equilibrium points.
3. Repeat Steps 1 and 2 at the new equilibrium and for the new set of parameters.
4. Repeat Steps 1, 2, and 3 until  $\lambda$  decreased by  $\delta\lambda$  or until the maximum number of iterations  $n_{ite}$  is exceeded.

### C. Saddle location control by local sensitivity analysis

Let  $x_0$  be a stable equilibrium of model (10) with parameters  $\pi$  and let Assumption IV.1 hold. Let  $s \in \mathbb{R}^n$  be a saddle point whose unstable manifold  $\mathcal{M}_s^u$  connects to  $x_0$ . Let

$$g_{s-x_0}(\pi) = \|s - x_0\| \quad (13)$$

be the Euclidean distance between the saddle and the stable point as a function of the model parameter. By the chain rule  $\frac{\partial g_{s-x_0}}{\partial \pi_i} = 2(s - x_0)^T \left( \frac{\partial s}{\partial \pi_i} - \frac{\partial x_0}{\partial \pi_i} \right)$ , where  $\frac{\partial s}{\partial \pi_i}$  and  $\frac{\partial x_0}{\partial \pi_i}$  can be computed as in Lemma IV.1. It follows that the distance between  $s$  and  $x_0$  is maximally increased along

$$d_{g_{s-x_0}} = \frac{\nabla g_{s-x_0}}{\|\nabla g_{s-x_0}\|} \quad (14)$$

where  $\nabla g_{s-x_0} = \left[ \frac{\partial g_{s-x_0}}{\partial \pi_1}, \dots, \frac{\partial g_{s-x_0}}{\partial \pi_m} \right]$ . Given (14), we can formulate fully-actuated and underactuated saddle location control strategies to increase  $g_{s-x_0}(\pi)$  by  $\delta g > 0$  units.

### Control Strategy IV.3. Fully-Actuated Saddle Control

1. Compute (12) at the current equilibrium and parameter values.
2. Update the parameters:  $\pi \leftarrow \pi + \varepsilon d_{g_{s-x_0}}$  and compute the new equilibrium points.
3. Repeat Steps 1,2 at the new equilibrium and for the new set of parameters.
4. Repeat Steps 1 and 2 until  $g_{s-x_0}(\pi)$  increased by  $\delta g$  or until the maximum number of iterations  $n_{ite}$  is reached.

Let  $\mathcal{K}_\pi$  the affine cone of admissible parameter directions.

### Control Strategy IV.4. Underactuated Eigenvalue Control

1. Compute  $\tilde{d}_{g_{s-x_0}} = \arg \max_{d \in \mathcal{K}_\pi} \frac{\langle d, d_{g_{s-x_0}} \rangle}{\|d\|}$  at the current equilibrium and parameter values.
2. Update the parameters:  $\pi \leftarrow \pi + \varepsilon d$ , and compute the new equilibrium points.
3. Repeat Steps 1 and 2 at the new equilibrium and for the new set of parameters.
4. Repeat Steps 1, 2, and 3 until  $g_{s-x_0}(\pi)$  increased by  $\delta g$  or until the maximum number of iterations  $n_{ite}$  is reached.

### D. Parameter sensitivity

The entries of the parameter control vectors  $d_\lambda$  and  $d_{g_{s-x_0}}$ , or their underactuated versions  $\tilde{d}_\lambda$  and  $\tilde{d}_{g_{s-x_0}}$ , provide the sensitivity of the applied control to the parameters. Control is highly sensitive to parameters associated to entries with large absolute value: small variations of those parameters have large effects on the controlled quantity. Control is weakly sensitive

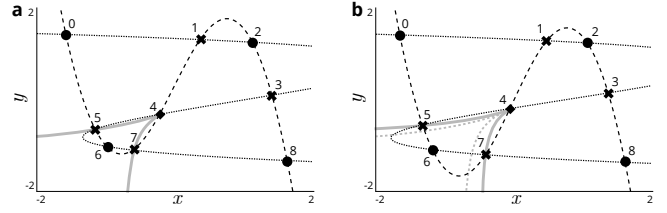


Fig. 4: Phase portrait of model (15) for nominal parameters (a) and for parameters controlled to enhance the stability and the size of the basin of attraction of equilibrium 6 (b). Stable steady-state are marked with circles, saddle points with crosses, and unstable points with diamonds.  $x$ -nullcline is dashed.  $y$ -nullcline is dotted. Saddle stable manifolds are in gray (only depicted for saddle points 5 and 7). In **b**, the stable manifolds from **a** are reproduced in dashed gray for comparison: the basin of attraction of equilibrium 6 is larger in **b** as compared to **a**.

to parameters associated to entries with small absolute value: big variations of those parameters are needed to affect the controlled quantity. In practice, highly sensitive parameters define the targets of experimental manipulations to bring a system to a desired state.

### E. Multi-objective control

A situation we will encounter in which the fully-actuated Control Strategies IV.1 and IV.3 are not feasible is when two or more eigenvalues, two or more saddles, or a mixture of them are simultaneously controlled. In those cases, a powerful way to implement the underactuated Control Strategies IV.2 and IV.4 is by using Multiple-Gradient Descent Algorithm (MGDA) methods [10], which returns an optimal constrained parameter control direction  $\tilde{d}$ . We will use this strategy in the numerical examples below.

#### F. A Two-dimensional Example

Consider the following two-dimensional dynamics

$$\begin{aligned} \dot{x} &= -x^{n_x} + \alpha_x \tanh(x) - y + u_x \\ \dot{y} &= -y^{n_y} + \alpha_y \tanh(y) - x + u_y \end{aligned} \quad (15)$$

with  $n_x, n_y \in \mathbb{N}$ ,  $\alpha_x, \alpha_y, u_x, u_y \in \mathbb{R}$ , which is a gradient dynamics with gradient function  $V_{n_x n_y}(x, y, \pi) = \frac{x^{n_x+1}}{n_x+1} + \frac{y^{n_y+1}}{n_y+1} - \alpha_x \ln |\cosh(x)| - \alpha_y \ln |\cosh(y)| + xy - u_x x - u_y y$ ,  $\pi = (\alpha_x, \alpha_y, u_x, u_y)$ . Observe that the two exponents  $n_x, n_y$  are not controllable parameters. They are fixed to  $n_x = 3$  and  $n_y = 5$  in what follows.

Figure 4, left, shows the phase portrait of model (15) for nominal parameter values ( $\pi = (3.0, 4.0, 0.3, 1.0)$ ). Our goal is to enhance the stability and increase the basin of attraction of equilibrium 6. More precisely, we want to decrease both eigenvalues  $\lambda_1, \lambda_2$  of the linearization of model (15) at equilibrium 6 by at least one unit. We apply Control Strategy IV.2 through MGDA [10] to simultaneously descend the gradient associated to the two eigenvalues. The two used control hyperparameters are  $\varepsilon = 10^{-2}$  and  $n_{ite} = 1000$ .

Figure 5 shows the action of our control strategy. Both controlled eigenvalues decrease along control iterations as

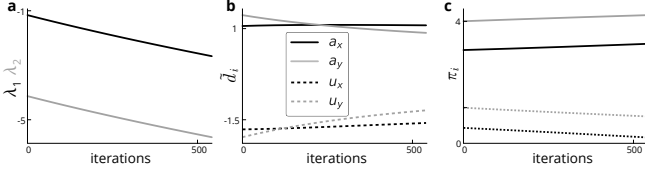


Fig. 5: **a.** Evolution of the two eigenvalues of equilibrium 6 as a function of control iterations. **b.** Evolution of the component of the sensitive parameter control direction  $\tilde{d}$ . **c.** Evolution of the components of parameter vector  $\pi$ . **b,c.** The association between line color/style and parameters of model (15) is indicated in the legend.

desired (Figure 5, left). The control goal is achieved in 544 iterations. As predicted by our theory, the parameter control signal also increases the size of the basing of attraction of equilibrium 6, as determined by the stable manifolds of saddle points 5 and 6 (Figure 4, right). Tracking the evolution of the computed parameter control direction across iterations reveals the control parameter sensitivity (Figure 5, center; see Section IV-D). The resulting evolution of the controlled parameters is shown in Figure 5, right.

## V. CONTROL OF THE EMT REGULATORY NETWORK

Multistable networks like molecule and gene regulatory networks are described using a variety of *qualitative* modeling approaches, like boolean networks [11] and piece-wise linear models [12]. Data is indeed often unavailable to derive detailed quantitative models. The goal of qualitative models is mainly to capture binary molecular interactions and the transitions between different discrete cellular states. As suggested by [13], there is however a middle-ground between purely qualitative and detailed quantitative modeling, in which smooth ordinary differential equation (ODEs) models are not fitted to experimental data but, even so, variables and governing parameters remain quantitative. This allows a finer understanding of the model dynamics and, crucially, of the effect that variations of biologically relevant parameters have on them beyond all-or-none harsh manipulations like gene knock-in and knock-out.

### A. Model derivation

Using boolean model reduction methods [14], [15], [16], it is possible to reduce the 9-dimensional boolean EMT model proposed in [17] to four boolean variables, evolving according to the boolean difference equation (16), while preserving the key genes and all the attractors of the full model (Table I). Model (16) can be translated to a parameterized system of differential equations by mapping boolean operators to sum and products of increasing or decreasing sigmoidal functions. We use Hill functions  $H(x, p, k) = \frac{x^p}{x^p + k^p}$  for increasing sigmoids and  $\bar{H}(x, p, k) = 1 - H(x, p, k)$  for decreasing sigmoids. With these choices, we can map boolean operators to elementary algebraic operations between sigmoids:

$$\begin{aligned} \neg x &\mapsto \bar{H}(x, p, k), & x \wedge y &\mapsto H(x, p_x, k_x)H(y, p_y, k_y) \\ x \vee y &\mapsto H(x, n_x, k_x) + H(y, n_y, k_y) \end{aligned}$$

Furthermore each interaction term is assumed to be parameterized by an interaction strength  $\alpha$ , and each variable has

TABLE I: Four-dimensional reduction of the boolean model in [17] and associated boolean epithelial, senescent, and mesenchymal attractors.  $\tau$  is the model discrete time.  $\neg$  denotes the boolean NOT operation.  $\wedge$  denotes the boolean AND operation.  $\vee$  denotes the boolean OR operation. .

$$\begin{aligned} S(\tau + 1) &= \neg E(\tau) \vee (S(\tau) \wedge E(\tau) \wedge N(\tau)) \\ E(\tau + 1) &= \neg S(\tau) \vee (S(\tau) \wedge E(\tau) \wedge \neg N(\tau)) \\ N(\tau + 1) &= S(\tau) \vee E(\tau) \vee N(\tau) \vee P(\tau) \\ P(\tau + 1) &= \neg S(\tau) \wedge ((E(\tau) \wedge N(\tau)) \vee P(\tau)) \end{aligned} \quad (16)$$

Gene (variable)	Epithelial	Senescent	Mesenchymal
<i>Snai2</i> (S)	0	0	1
<i>ESE2</i> (E)	1	1	0
<i>NFKB</i> (N)	1	1	1
<i>p16</i> (P)	0	1	0

a *linear degradation* term  $-x$  and a constant *source term*  $\beta$ . The proposed translation from boolean to smooth ODEs is similar in spirit to [18] but with the crucial difference that interaction strengths and half-activations are parameterized, and that the smooth variables are not assumed to live in a unitary hypercube. The resulting quantitative dynamics are

$$\begin{aligned} \frac{dS}{dt} &= \alpha_1 \frac{k_1^p}{E^p + k_1^p} + \alpha_2 \frac{S^p}{S^p + k_2^p} \frac{E^p}{E^p + k_3^p} \frac{N^p}{N^p + k_4^p} + \beta_S - S \\ \frac{dE}{dt} &= \alpha_3 \frac{k_5^p}{S^p + k_5^p} + \alpha_4 \frac{E^p}{E^p + k_6^p} \frac{S^p}{S^p + k_7^p} \frac{k_8^p}{N^p + k_8^p} + \beta_E - E \\ \frac{dN}{dt} &= \alpha_5 \frac{S^p}{S^p + k_9^p} + \alpha_6 \frac{E^p}{E^p + k_{10}^p} + \alpha_7 \frac{N^p}{N^p + k_{11}^p} + \alpha_8 \frac{P^p}{P^p + k_{12}^p} \\ &\quad + \beta_N - N \\ \frac{dP}{dt} &= \alpha_9 \frac{k_{13}^p}{S^p + k_{13}^p} \left[ \alpha_{10} \frac{E^p}{E^p + k_{14}^p} \frac{N^p}{N^p + k_{15}^p} + \alpha_{11} \frac{P^p}{P^p + k_{16}^p} \right] \\ &\quad + \beta_P - P \end{aligned} \quad (17)$$

In the limit  $p \rightarrow \infty$ , Hill functions become binary activation functions and model (17) becomes piece-wise linear, as in [12]. For finite  $p$ , the behavior remains quantitative, i.e., interaction terms varies smoothly with the model variables.

### B. Control through local sensitivity

For the nominal set of parameters  $\pi$  (see details at [19]) there are 3 stable points, corresponding to the epithelial, senescent, and mesenchymal phenotypes, respectively, 3 saddle points separating their basins of attraction, and 1 unstable point.

Our goal is to increase the size of the basin of attraction of the epithelial equilibrium  $x_e^*$ . We do so by computing through MGDA the sensitive direction in the parameter space that simultaneously *i*) makes more negative the two eigenvalues of  $J_{x_e^*}^\pi$  whose eigenvectors are tangent to the unstable manifolds of the saddle points surrounding  $x_e^*$  and *ii*) increase the average distance  $\overline{g_{x_e^* - s_{123}}}$  between  $x_e^*$  and the three saddle points delimiting its basin of attraction. The control iteration stopping criteria is that all stable equilibria are maintained, i.e., none of them disappear in a bifurcation.

The effects of the applied control strategy are summarized in Figure 6. Both controlled eigenvalues (Figure 6a) and  $\overline{g_{x_e^* - s_{123}}}$  (Figure 6b) change in the desired direction across control iterations. As a consequence and as predicted by our theory, the size of the basin of attraction<sup>2</sup> of  $x_e^*$  is largely increased (Figure 6c), that of the senescent equilibrium shrinks

<sup>2</sup>Computed through a Monte Carlo on initial conditions in  $[0, 4]^4$ .

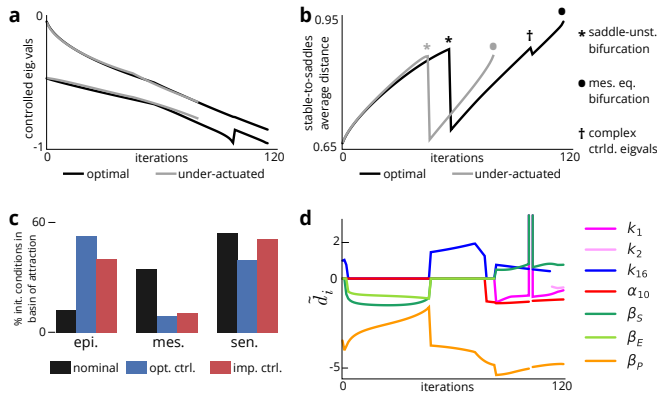


Fig. 6: **a.** Evolution of the two controlled eigenvalues across control iterations. **b.** Evolution of the average distance between  $x_e^*$  and saddle points delimiting its basin of attraction. **c.** Size of the basin of attraction of the three stable equilibria before (black) and after either the optimal control (blue) or the imperfect control (red) is applied. **d.** Components of the sensitive parameter control direction associated to the most sensitive parameters.  $\bullet$ : bifurcation of the mesenchymal stable equilibrium.  $*$ : bifurcation of one of the saddle delimiting the basin of attraction of  $x_e^*$  with an unstable equilibrium.  $\dagger$ : non-zero imaginary parts of the controlled eigenvalues.

slightly, and that of the mesenchymal equilibrium is reduced to approximately a third of its original size. The abrupt drops in the evolution of  $\overline{g_{x_e^* - s_{123}}}$  correspond either to bifurcations of the model equilibria or to some eigenvalues becoming complex (see Figure 6 for details).

Tracking the evolution of the components of the sensitive parameter control direction (Figure 6d) reveals the key parameters to be manipulated and whether they should be increased or decreased. For instance, initially the three source terms ( $\beta_i$ ,  $i = S, E, P$ ) must all be decreased. Subsequently, the half-activation  $k_{16}$  must be increased and interaction gain  $\alpha_{10}$  decreased. These parameter manipulations are highly counter-intuitive and hard to imagine or derive with a more heuristic approach.

To test the robustness and practical applicability of our control strategy, we assumed that only three out of 32 parameters with the largest absolute sensitivity could be manipulated at each control iteration, a kind of *under-actuated* control. As summarized in Figures 6a,b,c, although a slight drop in performance can be detected, the control goal is robustly achieved.

## VI. CONCLUSIONS

We derived a parameter control law to control the size and depth of the basins of attraction of a multistable dynamics with simple attractors. Our control law is cheap to compute because it solely use local information of the model dynamics at stable and saddle points. When applied to multistable biological models, like models of molecular regulatory networks underlying cellular decision making, our approach is able to suggest counter-intuitive parameter manipulations that can be tested in experimental settings to achieve desired control objectives. We illustrated this fact on the control of a new ODE model of

the epithelial-mesenchymal transition, with relevance for the control of tumor formation and metastasis.

## REFERENCES

- [1] A. N. Pisarchik and U. Feudel, "Control of multistability," *Physics Reports*, vol. 540, no. 4, pp. 167–218, 2014.
- [2] A. Bizyaeva, A. Franci, and E. L. Naomi, "Nonlinear opinion dynamics with tunable sensitivity," *To appear in IEEE Trans. Aut. Contr.*, 2022.
- [3] G. Balázsi, A. Van Oudenaarden, and J. J. Collins, "Cellular decision making and biological noise: from microbes to mammals," *Cell*, vol. 144, no. 6, pp. 910–925, 2011.
- [4] M. A. Nieto, R. Y.-J. Huang, R. A. Jackson, and J. P. Thiery, "EMT: 2016," vol. 166, no. 1, pp. 21–45.
- [5] J. Yang and R. A. Weinberg, "Epithelial-mesenchymal transition: At the crossroads of development and tumor metastasis," vol. 14, no. 6, pp. 818–829.
- [6] R. Chakrabarti *et al.*, "Elf5 inhibits the epithelial–mesenchymal transition in mammary gland development and breast cancer metastasis by transcriptionally repressing snail2," vol. 14, no. 11, pp. 1212–1222.
- [7] D. Efimov, "Global Lyapunov analysis of multistable nonlinear systems," *SIAM Journal on Control and Optimization*, vol. 50, no. 5, pp. 3132–3154, 2012.
- [8] M. Hirsch and S. Smale, *Differential Equations, Dynamical Systems, and Linear Algebra*. Academic Press: New York, 1974.
- [9] H. L. Smith, *Monotone dynamical systems*. American Mathematical Soc., 2008.
- [10] J.-A. Désidéri, "Multiple-gradient descent algorithm (mgda) for multi-objective optimization," *Comptes Rendus Mathématique*, vol. 350, no. 5-6, pp. 313–318, 2012.
- [11] R. Somogyi and C. A. Sniegoski, "Modeling the complexity of genetic networks: understanding multigenic and pleiotropic regulation," *complexity*, vol. 1, no. 6, pp. 45–63, 1996.
- [12] H. De Jong, J.-L. Gouzé, C. Hernandez, M. Page, T. Sari, and J. Geiselmann, "Qualitative simulation of genetic regulatory networks using piecewise-linear models," *Bulletin of mathematical biology*, vol. 66, no. 2, pp. 301–340, 2004.
- [13] N. Le Novère, "Quantitative and logic modelling of molecular and gene networks," *Nature Reviews Genetics*, vol. 16, no. 3, pp. 146–158, 2015.
- [14] M. T. Matache and V. Matache, "Logical reduction of biological networks to their most determinative components," *Bulletin of mathematical biology*, vol. 78, no. 7, pp. 1520–1545, 2016.
- [15] A. Veliz-Cuba, "Reduction of boolean network models," *Journal of theoretical biology*, vol. 289, pp. 167–172, 2011.
- [16] A. Saadatpour, R. Albert, and T. C. Reluga, "A reduction method for boolean network models proven to conserve attractors," *SIAM Journal on Applied Dynamical Systems*, vol. 12, no. 4, pp. 1997–2011, 2013.
- [17] L. F. Méndez-López, J. Davila-Velderrain, E. Domínguez-Hüttlinger, C. Enríquez-Olguín, J. C. Martínez-García, and E. R. Alvarez-Buylla, "Gene regulatory network underlying the immortalization of epithelial cells," *BMC systems biology*, vol. 11, no. 1, pp. 1–15, 2017.
- [18] L. Mendoza and I. Xenarios, "A method for the generation of standardized qualitative dynamical systems of regulatory networks," *Theoretical Biology and Medical Modelling*.
- [19] R. Moreno-Morton, "Stability control by local sensitivity analysis," *GitHub*: <https://github.com/rodrigo-moreno/basin-control-notebook>, 2022.